Int J Adv Manuf Technol (2015) 80:3–10
DOI 10.1007/s00170-015-6987-4

ORIGINAL ARTICLE

# Keyhole-induced porosity in laser-arc hybrid welded aluminum

**O. T. Ola · F. E. Doern**

Received: 27 October 2014 / Accepted: 2 March 2015 / Published online: 17 March 2015


**Abstract** Keyhole-induced macro-porosity, which results from the collapse of the keyhole that formed by the reaction forces of metal vapors, is a major problem limiting laser and laser-arc hybrid weldability of age-hardenable aluminum alloys, such as AA2024-T3. The mechanism of porosity suggests that the weld metal solidifies more rapidly than the possible rise velocity of the gas bubbles that formed during keyhole collapse, resulting in severe porosity. The porosity behavior of AA2024-T3 during laser-arc hybrid welding was studied using microscopy and X-ray radiography techniques. Porosity-free welding of the alloy is attainable in the conduction mode welding, whereas porosity increased significantly with increased laser intensity during keyhole mode welding. Porosity was mostly severe when the beam was focused at the surface of the workpiece. The laser beam and the arc decouple from each other with increased laser-wire distance, affecting keyhole depth and porosity. In order to control porosity during laser-arc hybrid welding of aluminum alloys, the role of various welding parameters on the material's response should be balanced with the required weld geometry.

**Keywords** Laser hybrid · Porosity · Aluminum alloys · Weldability · Keyhole · X-ray radiography

## 1 Introduction

Precipitation-strengthened aluminum alloys such as the 2000 and 7000 series alloys continue to be used for various structural applications in aerospace, automotive, and other industries due to their specific strength. Fabrication of complex components usually requires a method or a combination of methods of joining. Welding of various parts during fabrication is a common practice. Advancement in welding research led to the development of high-power beam techniques such as laser and electron beam welding with lower heat input and deeper weld penetration characteristics. Recent developments in the welding of precipitation-strengthened aluminum alloys show that laser welding of this class of alloys is becoming increasingly attractive [1–3]. An even more advanced method simultaneously combines a laser beam and an electric arc in what is referred to as laser-arc hybrid welding, making use of the synergy between the two heat sources in achieving advantages such as increased weld penetration and increased filler metal deposition rate, improved gap and misalignment tolerance, enhanced process stability, and improved overall weld quality [4–7].

Although the laser-arc hybrid welding technique provides a revolutionary way of joining materials by combining the advantages of laser welding and arc welding, studies have shown that precipitation-strengthened 2000 and 7000 series aluminum alloys usually exhibit weldability problems during welding [8–11]. One of the major problems during keyhole mode laser and laser-arc hybrid welding of the alloys is their susceptibility to macro-porosity in the weld metal. Macro-porosity during laser welding has been attributed to the instability of the keyhole formed by intense evaporation of materials during laser-material interaction [12, 13]. Keyhole-induced porosity is different from hydrogen-induced porosity [11, 14], which is more microscopic in nature, and interdendritic porosity [15] that have been reported by other researchers. Porosity during welding of materials can result in loss of mechanical strength and creep, fatigue, and corrosion failures [16, 17].

O. T. Ola (✉) · F. E. Doern
School of Transportation, Aviation and Manufacturing, Red River College of Applied Arts, Science and Technology, 2055 Notre Dame Ave., Winnipeg, MB R3H 0J9, Canada
e-mail: oola@rrc.ca

The mechanism of macro-porosity during high-power beam welding is somewhat understood. However, a review of the current state of research on porosity formation during keyhole laser and laser-arc hybrid welding of aluminum alloys suggests that optimization of the welding processes requires the acquisition of more data on the various factors contributing to porosity and the development of an approach to eliminate or significantly mitigate this problem. In this present work, the authors discuss the mechanism of macro-porosity and present their evaluation of the porosity response of AA2024-T3 during laser-arc hybrid welding. A possible approach for controlling porosity in the alloy is suggested. The results are elucidated in this article.

## 2 Materials and methods

The materials used in this study are AA2024-T3 welding coupons (base alloy) and $AlSi_5$ (ER4043) welding wire. The welding coupons were received in the form of plates having dimensions approximately 125 mm×50 mm×6 mm, while the 0.89-mm diameter welding wire was received in the form of a spool. The compositions of the base alloy and the welding wire are presented in Table 1. The surfaces of the welding coupons were ground using silicon carbide papers in order to remove surface oxides. The coupons were then subsequently cleaned with acetone. The welding equipment used consists of a 6-kW continuous wave Y-YAG laser and a Fronius 500-amp gas metal arc (GMA) welder integrated in the laser-arc hybrid welding configuration. The welding system was automated using a Yaskawa Motoman HP50 6-axis robot. All welds were made as bead-on-plates using the welding parameters listed in Table 2.

In order to analyze porosity in the weldments, X-ray radiography was carried out using a VJ Technologies X-ray system. The X-ray source was operated at 130 kV and 5 mA. Radiographs were produced from two planes at right angles to each other, parallel to the welding direction. Approximate diameters of pores were determined from the radiographs. The welded coupons were sectioned transverse to the welding direction for microstructural analysis. The weld sections were prepared using standard metallographic procedures. In order to reveal the fusion boundaries and the microstructure of the welds, the specimens were chemically etched by immersion in Keller's reagent for 30 s. They were then analyzed using a Nikon SMZ800 optical microscope equipped with NIS-Elements D imaging software and a Hitachi TM1000 scanning electron microscope (SEM). The dimensions of the weld beads were determined using the optical microscope and used alongside the approximate diameters of the pores to estimate the percent porosity in the weld metal.

**Table 1** Chemical compositions of the base alloy and the welding wire (weight percent)

| Alloy | Si | Fe | Cu | Mn | Mg | Cr | Zn | Ti | Al |
|---|---|---|---|---|---|---|---|---|---|
| AA2024 | 0.5 | 0.5 | 4.9 | 0.9 | 1.8 | 0.1 | 0.3 | 0.2 | Bal. |
| ER4043 | 5.0 | 0.8 | 0.3 | 0.1 | 0.1 | - | 0.1 | 0.2 | Bal. |

**Table 2** Welding process settings and parameters

| Welding parameters | |
|---|---|
| Filler wire | ER4043 |
| Wire diameter | 0.89 mm |
| Laser power | 2.5, 3.0, 3.7, and 4.0 kW |
| Laser focus | −2, −1, 0, 1, and 2 mm |
| Process ordering | Laser leading |
| Laser-wire distance | 1, 2, 3, and 5 mm |
| Welding speed | 1.0, 1.5, 2.0, and 2.5 m $min^{-1}$ |
| Wire feed speed | 7 m $min^{-1}$ |
| Shielding gas | Argon |
| Shielding gas flow rate | 20 L $min^{-1}$ |

## 3 Results and discussion

### 3.1 Keyhole-induced porosity in the welds

X-ray radiographs that were taken from two perpendicular planes of a laser-arc hybrid welded AA2024-T3 material that was welded with a laser power of 4 kW are presented in Fig. 1, showing macro-porosity in the weld. Radiographs taken from perpendicular planes allow easy differentiation between porosities that may appear overlapping from only one direction. The radiograph at the top of the figure was taken from the top plane of the weld (designated as 0°), while the bottom radiograph was taken from the side of the weld in the transverse direction (designated as 90°). The macro-size pores are randomly distributed along the weld without any noticeable distribution pattern, and the pores could be approximated to be spherical in shape. A more detailed study of the porosity revealed that the average pore diameter, depending on the

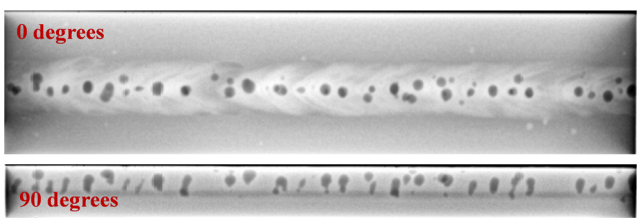


**Fig. 1** X-ray radiographs of an AA2024-T3 material that was laser-arc hybrid welded with a laser power of 4 kW

welding process conditions, could range from about 0.4 to 1.3 mm. Figure 2a is an optical image showing a macro-size pore of approximately 1.2-mm diameter in the weld metal of the laser-arc hybrid welded material. The SEM micrograph of Fig. 2b, which is the rectangular inset in Fig. 2a, shows the solidification microstructure of the weld metal at the boundary between the solidified metal and the pore that was completely devoid of solid materials. It was observed that the pores are either completely devoid of any solid material, as in Fig. 2a, b, or could be partially void with molten material somewhat encapsulated within the void, as in the SEM image of Fig. 2c. Nevertheless, excessive amount of porosity, such as observed in the laser-arc hybrid welded AA2024-T3 material in this present work, is known to limit components' lifetime by degrading the material's properties [12, 16, 17]. Therefore, it is important to develop an approach for reducing or totally eliminating porosity problems during laser and laser-arc hybrid welding. The development of a mitigation approach would require an adequate understanding of the mechanism and the factors influencing porosity during welding.

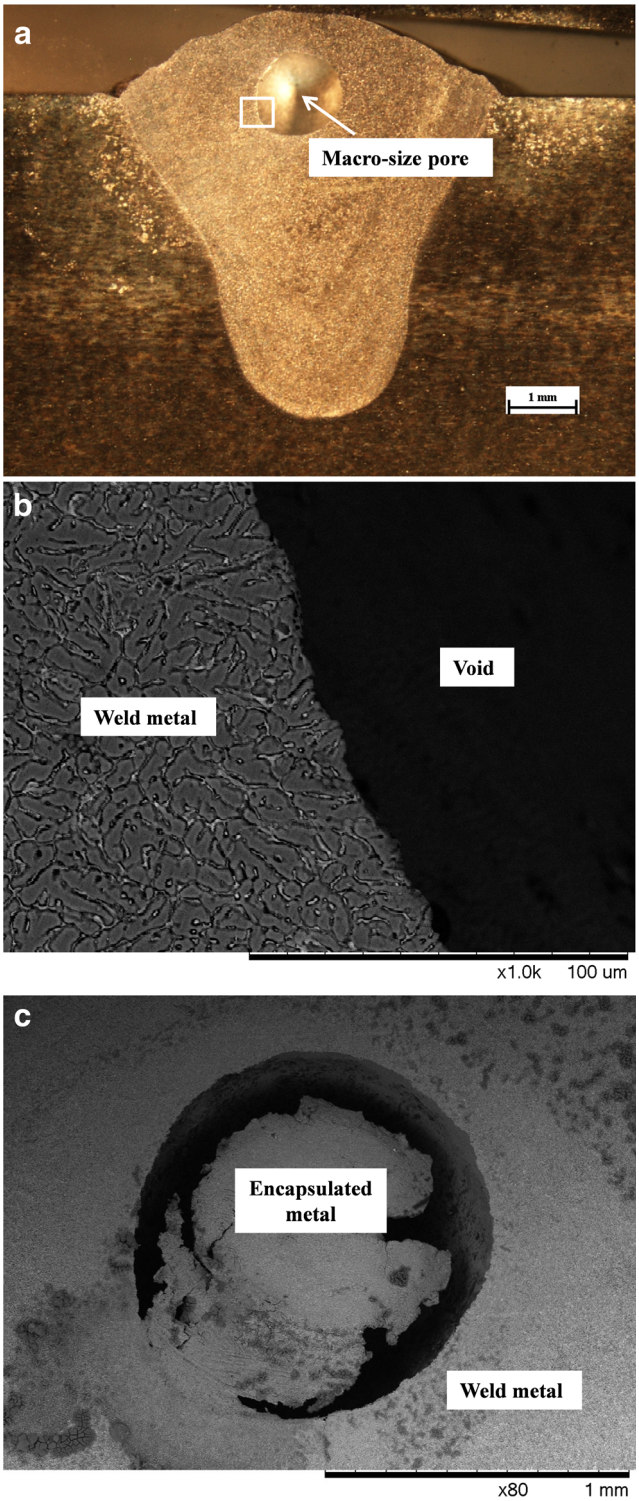


**Fig. 2** **a** Optical image showing an overview of a laser-arc hybrid weld in AA2024-T3 and a macro-size pore in the weld metal. **b** and **c** SEM micrographs showing the pore boundary (inset in (**a**) above) and a partially void pore, respectively

Irradiation of a metallic material by high-intensity laser beam could produce an amount of heat that is sufficient to break atomic bonds, thereby causing vaporization of the material and, in many cases, removal of electrons from the vaporized metal atoms and from gases in the interaction zone, resulting in plasma generation [18]. A keyhole eventually forms in the material under the influence of significantly high-intensity beam by the recoil pressure that pushes the surrounding molten material when the high-temperature vapor and plasma expand [18]. The keyhole is held open by the recoil pressure generated by this non-equilibrium evaporation of particles [19]. Earlier analysis of the nature of the keyhole suggested that the stability or collapse of the keyhole is dictated by the competition between different forces acting on the keyhole [19]. In the analytical study of quasi-static laser keyhole welding by Kroos et al. [19], the two major forces, among others, that were observed to provide the pressure balance required to maintain a stable keyhole are the ablation pressure, $P_{\mathrm{abl}}$, which tends to open the keyhole, and the surface tension forces, $P_{\gamma}$, which tends to close the keyhole. According to their analysis, $P_{\mathrm{abl}} \approx P_{\gamma}$ for iron and were suggested to be of the order of about $10^4$ Pa. The balance of pressures in the keyhole has also been expressed in a more recent work as [20]

$$P_{\mathrm{r}} + P_{\mathrm{v}} + \Delta P = P_{\gamma} + \rho_{\mathrm{l}} g h \tag{1}$$

The recoil pressure, $P_{\mathrm{r}}$, the vapor pressure, $P_{\mathrm{v}}$, and the gradient in pressure driving the vapor out of the keyhole, $\Delta P$, tend to maintain the keyhole, while the pressure due to surface tension effects, $P_{\gamma}$, and the hydrostatic pressure, $\rho_{\mathrm{l}} g h$ ($\rho_{\mathrm{l}}$ is the density of the liquid metal, $g$ is acceleration due to gravity, and $h$ is the depth of the keyhole) tend to close the keyhole.

Although the balance of forces could be useful for understanding the condition under which the keyhole may be stable, it is unlikely that this steady-state condition would exist in

reality during welding. The form and size of the keyhole varies according to external conditions including laser power, travelling speed, and material properties [19]. Studies have shown that the excessive pressure generated during keyhole welding induces temporal fluctuation and spatial instability of the keyhole, resulting in keyhole collapse and the entrapment of metal vapor and gases [10, 12, 13, 21]. It was observed that the size and shape of the keyhole fluctuated violently and, under this condition, large bubbles formed intermittently at the bottom of the keyhole and were trapped during solidification of the weld metal [13].

A generally held view is that delayed solidification by increase in heat input during welding could allow sufficient rise time of gas bubbles in the weld metal during welding, such that the gas bubbles escape before solidification [11, 22]. In this case, it would be expected that the rise time of the bubbles should be shorter than the time required for solidification of the molten weld pool. A simple treatment of the terminal velocity of a rising bubble in a fluid of known viscosity is given by Stoke's equation as [23]

$$V = g(d_F - d_B)D^2/18\nu \quad (2)$$

where $g$ is the gravitational acceleration, $d_F$ and $d_B$ are the densities of the fluid and the bubble, respectively, $D$ is the diameter of the bubble, and $\nu$ is the viscosity of the fluid. For a bubble of about 0.5-mm diameter in molten aluminum, Stoke's equation would have yielded a velocity of the order of 0.1 m $s^{-1}$, and assuming a keyhole depth of 4 mm, the bubble would have escaped in about 40 ms. Unfortunately, Stoke's equation is only valid for steady-state conditions. The state of the weld pool is usually turbulent and affected by other factors such as drastic temperature decrease and sharp loss of fluid viscosity, solidification, and the effect of shielding gases, which impede the motion of the bubble. Also, there is some evidence that the bubble velocity is suppressed during turbulent flow [24]. The solidification rate during laser welding of aluminum has been suggested to be up to $10^5$ °C $s^{-1}$ or higher [25, 26]. Under this condition, the weld metal solidifies more rapidly than the possible rise velocity of the gas bubbles formed during keyhole collapse, resulting in severe porosity in the weld metal.

In addition to the irradiation of the material by the laser beam, the electric arc also contributes in a synergic manner to the total amount of radiation in the keyhole during laser-arc hybrid welding. In laser-arc hybrid welding, both the laser beam and the electric arc simultaneously interact in the same process zone on the material. The intensity of the laser beam is usually of the order of $10^6$ W $cm^{-2}$, while the energy density of the freely burning arc could be up to $10^4$ W $cm^{-2}$ [5]. It is known that, during laser-arc hybrid welding, vaporization takes place from both the base alloy and the hot welding wire, such that more metal vapor is available in the keyhole [5]. The effect of this synergy, for the same laser power, is usually observed in the form of increased keyhole penetration during laser-arc hybrid welding compared to laser only [27]. Figure 3 is a schematic representation of a section along the weld bead during laser-arc hybrid welding, illustrating the contributions of the laser beam and the arc to keyhole behavior and the formation of macro-size pores in the weld metal. Detailed observation of the susceptibility of AA2024-T3 to porosity in this present work showed that any factor that influences keyhole behavior and causes a change in keyhole size would eventually affect porosity in the alloy. The influence of various laser-arc

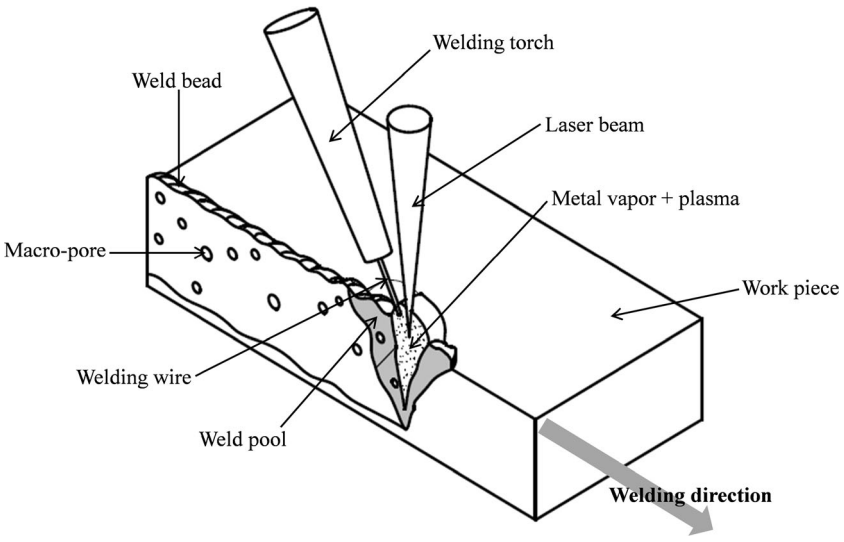


**Fig. 3** A schematic representation of a section along the weld bead during laser-arc hybrid welding

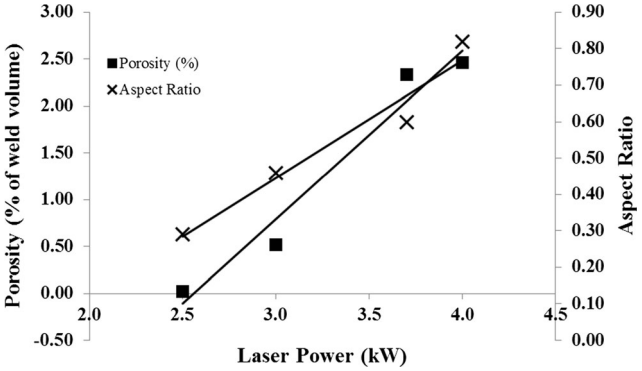


**Fig. 4** Weld aspect ratio and porosity as functions of laser power in laser-arc hybrid welded AA2024-T3

hybrid welding parameters on the keyhole, and the consequent effect on porosity, was studied. The results are discussed next.

### 3.2 The role of laser-arc hybrid welding parameters on porosity

Figure 4 shows the relationship between laser power and weld behavior of the laser-arc hybrid welded AA2024-T3. Increasing beam intensity by increasing laser power has the most effect on increasing the keyhole depth. The aspect ratio (depth-to-width ratio) increased dramatically for increasing laser power from 2.5 to 4 kW, when all other laser-arc hybrid welding parameters were kept constant. There was barely a keyhole at 2.5 kW, and the welding mode was essentially thermal conductive in nature. The thermal conductive nature of the welding mode at 2.5 kW resulted in a shallow weld (Fig. 5), with porosity hardly noticeable in the weld (Fig. 6). Porosity-free thermal conduction mode laser-arc hybrid welding is in agreement with the observation that keyhole collapse during welding is a major factor responsible for macro-porosity in welded aluminum alloys, as discussed

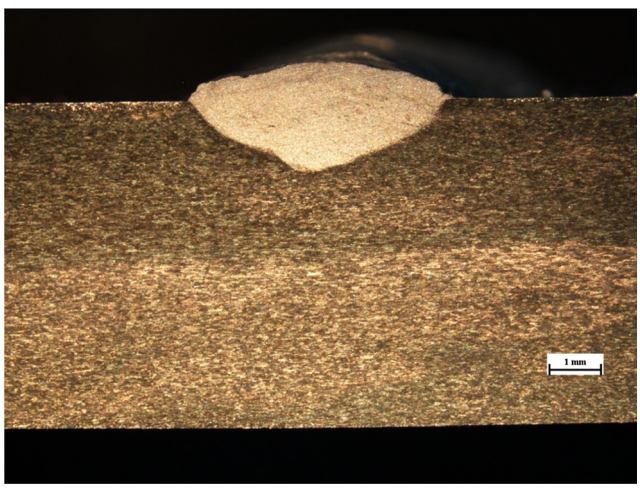


**Fig. 5** Optical image showing a thermal conduction mode laser-arc hybrid weld in AA2024-T3

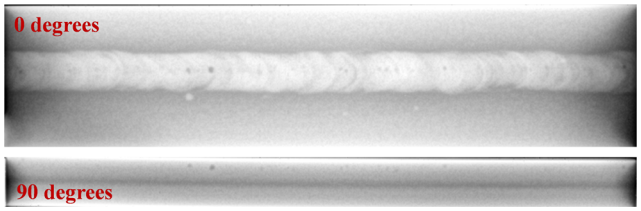


**Fig. 6** X-ray radiographs of a thermal conduction mode laser-arc hybrid weld in AA2024-T3, where porosity is hardly noticeable

earlier. However, as the laser power increased, porosity was observed to increase significantly (Fig. 4). It was observed that the average pore diameter, which is one of the criteria used for weld qualification in the industry [28], also increased significantly with laser power (Fig. 7). Transition from thermal conduction mode to keyhole mode usually occurs when the laser power density exceeds a certain limit where significant evaporation takes place and the reaction force of the evaporated metal is sufficient to induce a keyhole in the material [10]. The laser beam heats the material directly through the keyhole. Increasing the intensity of the beam usually increases the depth of the keyhole, which, in turn, results in increased tendency for porosity as the keyhole collapses. A similar observation has been observed during laser welding of Type 304 stainless steel, where the tendency to form pores changed from none or micro-porosity to macro-porosity with increasing power [16]. This current result suggests that the choice of laser power during laser-arc hybrid welding of AA2024-T3, and possibly other aluminum alloys, would depend on a balance between the required depth of penetration and the tolerable amount of porosity in the welded material. Another factor that was observed to have reduced porosity in the material was the welding speed. Figures 8 and 9 show the effect of welding speed (at the same laser power) on the aspect ratio and porosity and the average pore diameter, respectively. The result revealed that, although increased welding speed resulted in decreased depth of penetration, the aspect ratio did not change significantly. However, increased welding speed produced reduction in both the percent porosity and the average pore diameter. Reduction in the overall size of the keyhole by

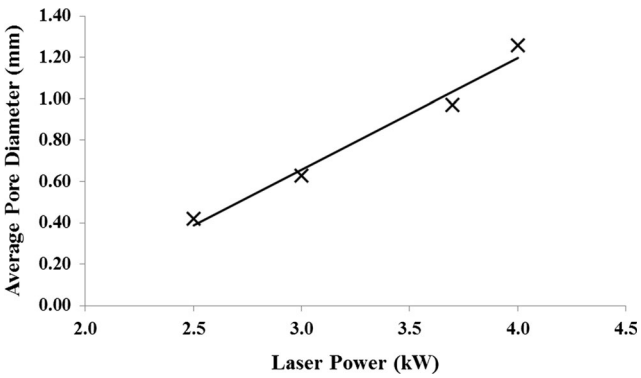


**Fig. 7** Average pore diameter as a function of laser power in laser-arc hybrid welded AA2024-T3

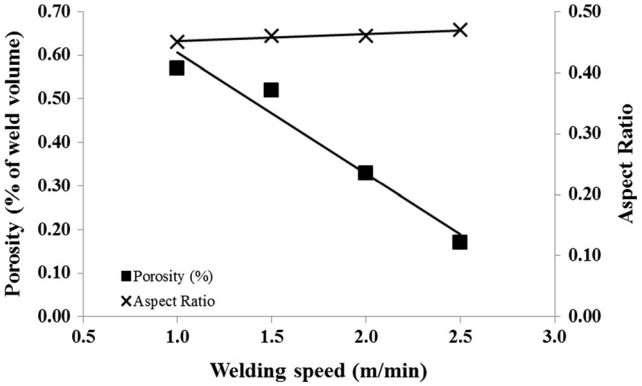


**Fig. 8** Weld aspect ratio and porosity as functions of welding speed in laser-arc hybrid welded AA2024-T3. Laser power=3 kW

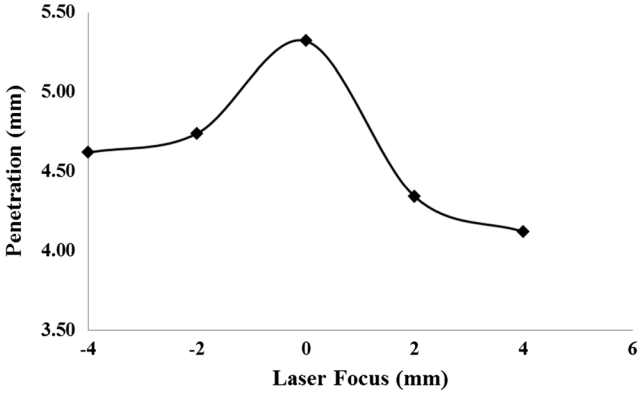


**Fig. 10** Weld penetration as a function of laser focal position in laser-arc hybrid welded AA2024-T3. Laser power=4 kW

increased welding speed is a factor that could have contributed to reduction in porosity in the alloy.

The role of laser focal position on porosity was studied. Defocussing the laser beam usually results in reduced penetration depth during welding [10], which was also observed in this present work (Fig. 10). Figure 10 suggests that defocussing the beam positively (above the workpiece surface) resulted in shallower penetration compared to defocussing negatively. The most severe porosity and the largest average pore diameter were observed in the material when the beam was focused at the surface of the workpiece. Porosity reduced with laser beam defocussing, and specifically, defocussing the beam positively was found to be more effective in reducing porosity compared to defocussing the beam negatively (Fig. 11). This is consistent with the observed effect of laser focal position on the depth of penetration during welding.

Previous analysis of laser-arc hybrid welding of materials showed that the synergy that results from the coupling of laser beam and electric arc during welding results in several advantages [5–7, 29]. The most obvious advantage, which has been reported by several researchers, is increased depth of penetration. Naito et al. [29] demonstrated that the penetration was deepest when the distance between the laser beam axis and the electrode was 2 mm during laser-tungsten inert gas welding, and then becomes shallower with increased distance between the two heat sources. Nevertheless, experimental data demonstrating the effect of laser-electrode distance on weld quality during laser-arc hybrid welding is scarce in the literature. In order to study the effect of the synergy between laser and arc during welding, the distance between the laser beam axis and the GMAW electrode (laser-wire distance) was varied from 1 to 5 mm. Figure 12 shows the relationship between the laser-wire distance and the depth of penetration. The result showed that the deepest penetration was achieved at a laser-wire distance of 2 mm. This is in agreement with the work of Naito et al. [29]. Although shallower penetration at 1-mm distance appears to be counterintuitive, it is possible that the filler wire interferes with the path of the beam during forward feeding of the wire when the laser-wire distance becomes too small. At a laser-wire distance of 5 mm, it was observed that the depth of penetration realized in the material (≈4.4 mm) was the same depth of penetration realized when laser beam alone was used for welding the alloy. It was concluded that the laser beam and the arc had decoupled from each other before the laser-wire distance of 5 mm under the welding condition that was studied. As shown in Fig. 12, a direct correlation was observed between the depth of penetration (as a result of laser-wire

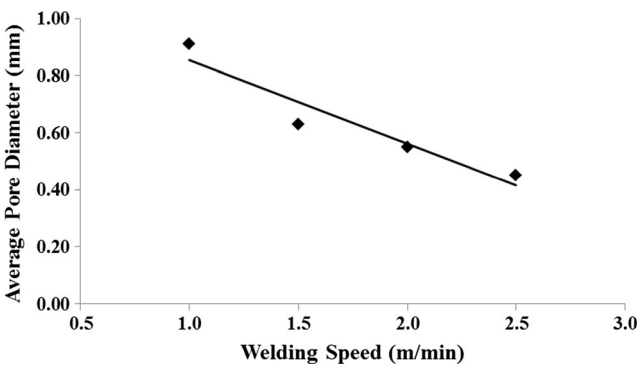


**Fig. 9** Average pore diameter as a function of welding speed in laser-arc hybrid welded AA2024-T3. Laser power=3 kW

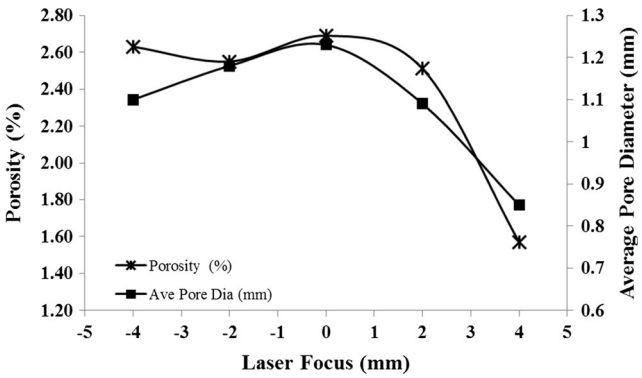


**Fig. 11** Porosity and average pore diameter as functions of laser focal position in laser-arc hybrid welded AA2024-T3. Laser power=4 kW

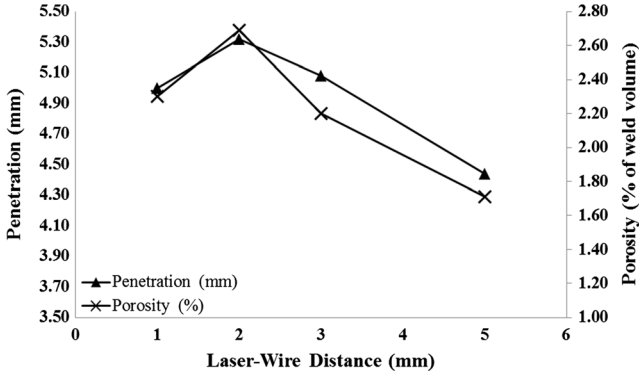


**Fig. 12** Penetration and porosity as functions of laser-wire distance in laser-arc hybrid welded AA2024-T3. Laser power=4 kW

distance) and porosity. This result reinforces the authors' observation that the addition of an electric arc to laser beam during laser-arc hybrid welding contributes to vaporization in the keyhole, with consequent increase in keyhole depth and the resultant increase in porosity. Therefore, in order to control porosity during laser-arc hybrid welding of aluminum alloys, the role of various welding parameters should be balanced with the required weld geometry.

## 4 Conclusions

The result of this work can be summarized as follows.

1. Severe keyhole-induced macro-porosity is one of the major factors that limit the applicability of laser-arc hybrid welding for fusion welding of AA2024-T3 and, possibly, other age-hardenable aluminum alloys.
2. Macro-porosity occurs in the weld metal when the solidification rate is faster than the rise velocity of the gas bubbles that formed as a result of the collapse of the keyhole.
3. Porosity-free laser-arc hybrid welding of the alloy is attainable in the conduction mode. However, as the welding mode transitions from conduction to keyhole mode, porosity increased significantly with increased laser intensity.
4. The most severe porosity was observed in the material when the beam was focused at the surface of the workpiece. Defocussing the laser beam was effective in reducing porosity.
5. The laser beam and the arc decouple from each other with increased laser-wire distance, and a direct correlation was observed between the depth of penetration and porosity.
6. The role of various welding parameters should be balanced with the required weld geometry in order to control porosity during laser-arc hybrid welding of aluminum alloys.

**Acknowledgments** The authors would like to thank Justin Grehan and Jess Caparros of StandardAero for their technical expertise in laser welding and X-ray radiography, respectively. The technical assistance of Minying Yao of Red River College is also gratefully acknowledged.

**Conflict of interest** The authors declare that they have no conflict of interest.

## References

1. Freeman R (2012) New welding techniques for aerospace engineering. In: Chaturvedi MC (ed) Welding and joining of aerospace materials. Woodhead Publishing Limited, Cambridge, pp 3–24
2. Allen CM, Verhaeghe G, Hilton PA, Haeson CP, Prangnell PB (2006) Laser and hybrid laser-MIG welding of 6.35 mm and 12.7 mm thick aluminium aerospace alloy. Mater Sci Forum 519–521:1139–1144
3. Molian PA, Srivatsan TS (1990) Weldability of aluminium-lithium alloy 2090 using laser welding. J Mater Sci 25(7):3347–3358
4. Steen WM, Eboo E (1979) Arc-augmented laser welding. Met Constr 11(7):332–335
5. Staufer H (2007) Laser hybrid welding in the automotive industry. Weld J 86:36–40
6. Mahrle A, Beyer E (2006) Hybrid laser beam welding—classification, characteristics, and applications. J Laser Appl 18:169–180
7. Ishide T, Tsubota S, Watanabe M, Ueshiro K (2003) Latest MIG, TIG arc-YAG laser hybrid welding system. J Jpn Weld Soc 72:22–26
8. Hu B, Richardson IM (2006) Hybrid laser/GMA welding aluminum alloy 7075. Weld World 50(7/8):51–57
9. Maamar H, Otmani RR, Fahssi T, Debbache N, Allou D (2008) Heat treatment and welding effects on mechanical properties and microstructure evolution of 2024 and 7075 aluminium alloys. Hradec nad Moravici - METAL 5:13–15
10. Kim JS, Watanabe T, Yoshida Y (1995) Effect of the beam-defocusing characteristics on porosity formation in laser welding. J Mater Sci Lett 14:1624–1626
11. Shtrikman MM, Pinskiia AV, Filatovb AA, Koshkinb VV, Mezentsevab EA, Guk NV (2011) Methods for reducing weld porosity in argon-shielded arc welding of aluminium alloys. Weld Int 25(6):457–462
12. Tucker JD, Nolan TK, Martin AJ, Young GA (2012) Effect of travel speed and beam focus on porosity in alloy 690 laser welds. JOM 64(12):1409–1417
13. Matsunawa A, Kim JD and Katayama S (1997) Porosity formation in laser welding-mechanisms and suppression methods. Int. Cong. on Applications of Lasers and Electro-Optics-ICALEO, 1997. Section G, Miami, p 73–82
14. Devletian JH, Wood WE (1983) Factors affecting porosity in aluminum welds—a review. Welding Research Council Bulletin 290, New York, pp 1–18
15. Kuo S (2003) Welding metallurgy, 2nd edn. Wiley, Hoboken
16. Norris JT, Robino CV, Hirschfeld DA, Perricone MJ (2011) Effects of laser parameters on porosity formation: investigating millimeter scale continuous wave Nd:YAG laser welds. Weld J 90:198s–203s
17. Daugherty WJ, Cannell GR (2003) Analysis of porosity associated with Hanford 3013 outer container welds. Pract Fail Anal 3(4):56–62
18. Reutzel EW (2009) Advantages and disadvantages of arc and laser welding. In: Olsen FO (ed) Hybrid laser-arc welding. Woodhead Publishing Limited, Cambridge, pp 3–27
19. Kroos J, Gratzke U, Simon G (1993) Towards a self-consistent model of the keyhole in penetration laser welding. J Phys D Appl Phys 26D: 474–480
20. Ribic B, Palmer TA, DebRoy T (2009) Problems and issues in laser-arc hybrid welding. Int Mater Rev 54(4):223–244

21. Kawahito Y, Mizutani M, Katayama S (2007) Elucidation of high power fibre laser welding phenomena of stainless steel and effect of factors on weld geometry. J Phys D Appl Phys 40:5854–5859
22. Zhou J, Tsai H-L (2007) Porosity formation and prevention in pulsed laser welding. Trans ASME 129:1014–1024
23. Wang LK, Shammas NK, Selke WA, Aulenbach DB (2010) Gas dissolution, release, and bubble formation in flotation systems. In: Wang LK (ed) Handbook of environmental engineering volume 12, flotation technology. Springer, New York, pp 49–83
24. Snyder MR, Knio OM, Katz J, Le Maitre OP (2007) Statistical analysis of small bubble dynamics in isotropic turbulence. Phys Fluids 19(6):1–68
25. Tu J, Paleocrassas A (2010) Low speed laser welding of aluminium alloys using single-mode fiber lasers. In: Xiaodong Na S (ed) Laser welding. Sciyo, InTech, Rijeka, pp 47–76, ISBN: 978-953-307-129-9
26. Cieslak MJ (1992) Phase transformations in weldments: new materials and new perspectives. 3rd Int. Conf. on Trends in Welding Research. ASM International, Gatlingburg, p 229
27. Ola OT, Ojo OA, Chaturvedi MC (2013) Laser arc hybrid weld microstructure in nickel based IN738 superalloy. Mater Sci Technol 29(4):426–438
28. American Welding Society (AWS) D17. Committee on Welding in the Aircraft and Aerospace Industries (2012) AWS D17.1—specification for fusion welding for aerospace applications. American Welding Society, Miami
29. Naito Y, Katayama S, Matsunawa A (2003) Keyhole behavior and liquid flow in molten pool during laser-arc hybrid welding. Proc SPIE Int Soc Opt Eng 4831:357–362